

Observation of metastable atomic nitrogen adsorbed on Ru(0001)

L. Diekhöner, A. Baurichter, H. Mortensen, and A. C. Luntz
Fysisk Institut, SDU-Odense Universitet Campusvej 55, DK-5230 Odense M, Denmark

(Received 1 September 1999; accepted 9 November 1999)

Exposing a Ru(0001) surface to an atomic beam of N produces a series of different states of atomic N adsorbed on the surface. For low atom doses, well-known low coverage states are produced, but for higher atom doses, several previously unknown higher coverage states are sequentially filled. These states exhibit well defined temperature programmed desorption (TPD) peaks which shift to considerably lower temperatures with N coverage. The highest N coverage obtainable is almost 1 ML N/Ru. Recent density functional calculations demonstrate that the N–Ru energy decreases significantly with N coverage, and in fact predict that N adsorbate states are not thermodynamically stable relative to associative desorption at high coverage. The observed high coverage states must, therefore, be metastable with lifetimes determined by the height of the barrier between gas phase N₂ and the adsorbed atomic states. Simple analysis of the TPD features in combination with the theoretical adsorption energies allows us to estimate these coverage dependent barrier heights. We find that the barrier heights increase significantly with coverage, and this is important in the metastability of the adsorbed states. A comparison of nitrogen adsorption on Ru(0001) with oxygen adsorption on Ru(0001) surface is stressed throughout. © 2000 American Institute of Physics. [S0021-9606(00)70705-7]

INTRODUCTION

There has been considerable interest in recent years in the interaction of both N₂ and O₂ with ruthenium surfaces. One motivation for this interest is the importance of these systems to catalysis; O₂/Ru for oxidation and N₂/Ru for the catalytic synthesis of ammonia. In the latter, ruthenium makes a more active (but more expensive) catalyst for NH₃ synthesis from N₂ and H₂ than the conventional reduced iron catalyst.¹ Although catalysts are in no sense well defined surfaces, there has been a long history of trying to build understanding based on chemistry at single crystal surfaces, and for Ru, the close packed Ru(0001) surface has been particularly well studied.

In some ways, the interaction of O₂ and N₂ with Ru(0001) are similar. Both break a strong diatomic bond and form strong adsorbate–Ru bonds in the process of dissociative chemisorption. Both N and O atoms adsorbed on Ru(0001) are strongly bound in hcp threefold sites,^{2–5} albeit with somewhat different long range structures at low coverage. Density functional theory (DFT) calculations show that the binding energies for both N and O on Ru(0001) decrease rather strongly with adsorbate coverage,^{2,4,6,7} indicating strong indirect adsorbate–adsorbate repulsive interactions. Because both O and N adsorbates interact strongly with the localized *d*-bands of the Ru, this decrease in binding energy at higher coverages has been interpreted as due to the need to “share” the limited Ru *d*-band electrons at higher coverage.⁶

There are of course significant differences between the interaction of the two species with Ru(0001) as well. Since the N–N bond is roughly 4.6 eV stronger than the O–O bond, the energetics and dynamics of dissociative chemisorption are considerably different between the two systems. Dissociation of O₂ on Ru(0001) is much more exothermic

than dissociation of N₂ on the surface. Also, the initial (zero coverage) dissociative chemisorption of O₂ is unactivated and proceeds through a molecular precursor mechanism,⁸ while the dissociative chemisorption of N₂ is strongly activated. Most theoretical estimates and measurements suggest that this barrier is ca. 1.4–2 eV at low N coverages.^{6,9,10} In addition, the N–N indirect repulsive interaction between adsorbed atoms^{4,6} is stronger than that for O–O adsorbed atoms,^{2,7} presumably because N has three valence electrons/atom interacting with the limited number of Ru *d*-band electrons instead of two valence electrons/atom for O.

The energetics and geometrical structure for a whole series of states with different O coverage (Θ_O) adsorbed on Ru(0001), up to $\Theta_O=1$, have recently been characterized.^{3,7,11,12} All are thermodynamically stable, although there is a “kinetic barrier” for forming the higher coverage states. While several lower coverage states for N adsorbed on Ru(0001) are now known, there has been uncertainty as to the existence of higher coverage states and the maximum N coverage achievable. Because of the very high barrier to N₂ dissociation, it is impossible to build up a high coverage of adsorbed N by direct dissociation of N₂ without major contamination. With a thermal dissociation probability as low as 10⁻¹² at room temperature, unreasonably long exposures and high pressures are required for background dosing. “Filament assisted” dissociation of N₂, which enhances the dissociative sticking by a factor of 10⁶, or decomposition of ammonia, followed by an anneal to a surface temperature $T_s=615$ K has been used to prepare the $p(2\times 2)-N$, $\Theta_N=0.25$ adlayer.^{13,14} Similarly, extensive exposure to ammonia followed by an anneal to $T_s=525$ K prepares the $(\sqrt{3}\times\sqrt{3})R-30^\circ-N$, $\Theta_N=0.33$ adlayer.¹⁴ Both have been well characterized by low energy electron diffraction (LEED).⁴ In

addition, a slightly higher N coverage of 0.36–0.44 was also obtained by decomposition of ammonia¹⁴ or hydrazine¹⁵ and corresponds to a so-called heavy domain wall structure (HDW). This structure is thought to be essentially patches of the $(\sqrt{3} \times \sqrt{3})R-30^\circ$ structure with higher density at the domain walls.^{14,15} An even higher N coverage has been obtained by decomposition of ammonia at surface temperatures in a sequence from 500 to 350 K, but because of the lower surface temperature much of the adsorbed N was in the form of NH_x fragments.¹⁴

In this article we show that by dosing with an atomic N beam, a series of different adsorbate N states can be prepared on the Ru(0001) surface. For low atom beam doses, the known $p(2 \times 2)-\text{N}$, $(\sqrt{3} \times \sqrt{3})R-30^\circ-\text{N}$, and HDW states are produced. However, for higher atom doses we find sequential filling of several previously unknown and lower stability high coverage states, ultimately saturating at a maximum coverage of ≈ 1 ML N/Ru atom. The results show a very large decrease in the thermal desorption peak temperatures with coverage so that these high coverage states would not be observable with surface temperatures used in previous experimental procedures to produce adsorbate coverages.

Recent DFT calculations for N adsorbed on Ru(0001) (Refs. 4,6,16) indicate that the higher coverage states are in fact not stable relative to associative desorption. The high coverage states must therefore be metastable, with a lifetime determined by the height of the barrier between gas phase N_2 and the adsorbed N states. Combination of our experimental TPD results with the DFT calculations allows us to estimate these coverage dependent barriers. We find that barriers increase significantly with N coverage and this is in fact a necessary aspect for the metastability of the highest coverage state.

EXPERIMENT

The experiments reported in this article were performed in a ultra-high vacuum (UHV) system, having a base pressure of 1×10^{-10} Torr. The system consists of a sample manipulator with a Ru(0001) sample, a differentially pumped quadrupole mass spectrometer for careful temperature programmed desorption (TPD) from the front surface of the crystal, an ion gun for sputter cleaning of the sample, Auger electron spectroscopy (AES) with a cylindrical mirror analyzer, low energy electron diffraction (LEED), an additional quadrupole mass spectrometer measuring the background gas in the chamber, a rotatable differentially pumped mass spectrometer, and a triply differentially pumped supersonic molecular beam. N dosing of the sample was accomplished via an active nitrogen ‘‘beam’’. A doubly differentially pumped H atom beam source was also used in the experiments. Much of this system has been described previously.¹⁷

The ruthenium crystal, 9 mm in diameter and 1 mm thick, was aligned and polished within 0.1° of the (0001) face. A groove was spark eroded on each side of the crystal, and the crystal was clamped by Ta pieces mounted onto a water cooled Cu block. A type C thermocouple was pressed into a small hole, spark eroded in the side of the crystal. The crystal was heated by electron bombardment on the back of

the crystal. The overall thermal time constant for cooling of the crystal (when thermal conductance dominated) was ca. 1 min.

The crystal was initially cleaned after introduction into vacuum by repeated heating cycles to 1500 K in oxygen (2×10^{-8} Torr) followed by flashes to 1600 K in UHV. Heating the sample in O_2 results in the removal of C in the form of CO, and annealing to 1600 K in UHV removes remaining chemisorbed oxygen. This is a standard cleaning procedure to remove C, the main chemical impurity, from the near surface region of Ru. After many such cycles, the sample was judged C-free in the near surface region by the absence of a CO desorption peak following saturated adsorption of background O_2 . AES is not sensitive to adsorbed C on Ru due to overlap of the C peak with a Ru peak.

Prior to each nitrogen adsorption experiment, this oxidation-anneal cycle was also repeated to insure that the sample was free of adsorbed C. Ar ion sputtering was also periodically included in the cleaning procedure. No features other than those attributed to Ru were observed by Auger analysis and indicates that chemical impurities on the surface are minimal. In particular, there was no observable Fe Auger signal, implying that this common bulk impurity in Ru was below detectable Auger limits for our sample.

In addition to the undetectable level of chemical impurities on our sample, we also believe the surface defect density was quite small. LEED at 300 K showed quite sharp substrate spots with a very low diffuse background. In addition, the specular reflectivity of a 300 K He nozzle atom beam from the surface at an incident angle of 27° relative to the surface normal was ~ 0.9 for a Debye Waller extrapolation to $T_s=0$ K. Since thermal He atom scattering is very sensitive to surface defects, this high He surface reflectivity also indicates a very low surface defect density. The surface defect density was estimated as 0.25% by CO titration. In this procedure, a 0.02 L (Langmuir) CO dose resulted not only in the usual CO TPD peak at ca. 500 K, but also a small shoulder at 575 K believed to be due to CO adsorbed at surface defects. The relative intensities of the two CO TPD features allowed an estimate of surface defect density, although the nature of these defects is unknown.

The active nitrogen beam for dosing of the Ru(0001) surface was produced by a microwave discharge (2.45 GHz, 50 W) in high purity N_2 (99.999%) at ca. 1 torr pressure in a 1 cm diameter quartz tube. Following the discharge, the active nitrogen flowed through a 250 mm length of 1.8 mm id capillary tubing into the UHV system and aimed at the Ru(0001) surface. The capillary tube, which ended some 80 mm in front of the crystal surface, acted as a single long channel beam source pointing at the crystal and provided modest collimation of the beam onto the sample. The pressure build up in the chamber was 1×10^{-7} Torr during nitrogen dosing. The internal of the capillary tube was coated with phosphoric acid to minimize heterogeneous recombination of atoms formed in the discharge on the tube walls as they flowed into the UHV chamber. The presence of N atoms in the capillary tube was evident from the characteristic emission of the nitrogen afterglow (formed by the gas phase recombination of nitrogen atoms). Unfortunately, some im-

purities are required to produce a significant concentration of atoms in discharge flow systems.¹⁸ Both the quartz discharge tube and the phosphoric acid added sufficient oxygen impurity for this purpose. As a result, the active nitrogen beam contained an unavoidable (and somewhat variable) oxygen impurity.

The active species from the microwave discharge that produces adsorbed N on the Ru(0001) surface is unknown with certainty. Discharges in N₂ can produce atoms at a few percent level, metastable molecular nitrogen, and vibrationally excited ground state molecules. Generally, metastable molecules are quenched in a pure N₂ discharge.¹⁹ The active nitrogen beam was also investigated by resonantly enhanced multiphoton ionization spectroscopy (REMPI) using the 2+1 ionization scheme with a laser wavelength of ca. 203 nm.²⁰ This sensitive spectroscopy, which vibrationally resolves the N₂, showed that no vibrationally excited species produced in the discharge survived the flow down the capillary tube into the vacuum system. We therefore assume that the active species forming adsorbed N on Ru(0001) is the atoms produced in the discharge. Assuming that the sticking coefficient of the atoms on the surface is unity, we estimate an atom flux at the surface of ~ 0.3 ML/min, $\sim 8 \times 10^{12}$ atoms/cm²/s from the initial build up of N atoms on the surface. This is consistent with an atom concentration in the beam of a few percent and is quite typical for dissociation probabilities quoted for pure N₂ discharges.

Because the N atom beam contained an oxygen atom impurity, initial experiments showed some build up of adsorbed oxygen as well as adsorbed N on the surface with extended beam exposures. We therefore developed a "scrubbing" procedure to remove the surface O without depleting significantly the surface N coverage. This scrubbing procedure was based on exposure of the surface with adsorbates to a H atom (D atom) beam. Gas phase H atoms react with adsorbed O via an Eley-Rideal reaction to form H₂O which readily desorbs from the surface (at $T_s > 200$ K).²¹ In a similar manner, gas phase H atoms react with adsorbed N atoms, presumably to form NH₃. Subsequent anneals of the surface to $T_s \geq 485$ K ensured that no H or NH_x remained on the surface after exposure to the H atom beam. The key fact that made the scrubbing feasible was that the removal rate by gas phase H atoms of adsorbed O was ca. 4 times greater than that for adsorbed N as measured by the disappearance of Auger peaks.

The H (or D) atom beam used in this scrubbing was formed by a microwave discharge in a manner similar to that for the N atom beam. The H (or D) atom beam, however, was well collimated by two stages of differential pumping to just expose the Ru(0001) surface. The dissociation efficiency for H₂ (or D₂) in microwave discharges is extremely high, and the beam striking the surface was $>50\%$ dissociated as determined by mass spectrometry of the direct collimated beam. The H (or D) atom flux at the surface was estimated as 0.015 ML/sec from the extent of dissociation and the overall beam flux at the surface (determined by sticking of H₂ relative to a background dose).

After dosing with the N atom beam, temperature programmed desorption (TPD) was performed using a differen-

tially pumped quadrupole mass spectrometer (QMS) with an orifice of 5 mm in diameter placed 2 mm from the sample. In this way we ensure that only species desorbing from the front surface are detected by the QMS. Typical linear heating rates of the sample were 3 K/s. Only mass 14 and 28 were significant peaks in the TPD after atom dosing. Both mass 28 and mass 14 showed the same behavior. In order to avoid confusion with any possible CO contamination peak, mass 14 was usually chosen for detection. To minimize CO adsorption during N atom dosing the surface temperature T_s was usually kept at 400 K. This T_s is above the desorption temperature of CO when N is also adsorbed on the surface.

RESULTS

Initial experiments involved simply looking at the N₂ TPD spectra (mass 14) following various dosing times from the atom beam. For low atom beam doses (0.5 min), a single and broad desorption feature centered at ca. 800 K is observed. This TPD feature is well-known from adsorption studies using filament assisted dissociation of molecular nitrogen¹³ and thermal decomposition of ammonia¹⁴ to result from the associative desorption of atomic nitrogen on the Ru(0001) surface. At higher atom doses, we find that a series of new states are sequentially populated and desorb at lower and lower surface temperatures. As we show below, the adlayers formed by exposure to only the N atom beam are somewhat contaminated by an O impurity so we will not discuss in detail here the TPD spectra. We simply note at this stage that due to an apparent increase in N coverage (or O coverage), N₂ desorption features were observed at significantly lower T_s . We will show in later experiments that both high coverage of N and coadsorption of large O coverage with the N each independently produce low T_s associative desorption peaks of N₂.

Auger measurements of the N (and O) coverage as a function of exposure time to the atom beam allowed us to follow the buildup of N (and O) quantitatively and is given in Fig. 1. The relative N coverage was measured by the intensity of the 379 eV N peak in the differentiated spectrum, to that of the 231 eV Ru peak, and the relative O coverage was measured by the intensity of the 503 eV peak to that of the 231 eV Ru peak. To calibrate the absolute N coverage, the Auger intensities were normalized assuming that the saturation adlayer obtained by extended NH₃ decomposition at 610 K is the $p(2 \times 2)$ -N, $\Theta_N = 0.25$ adlayer.⁴ This calibration agreed within 15% to that obtained comparing the N₂ TPD intensity to the CO TPD intensity from a CO saturated surface at $T_s = 300$ K ($\Theta_{CO} = 0.56$).²² The O coverage was calibrated by comparing Auger intensities to that of the $p(2 \times 1)$ adlayer ($\Theta_O = 0.50$) formed by saturated O₂ dissociative adsorption at 300 K. The ratio of the Auger sensitivities for N and O obtained independently was in good agreement with the ratio obtained by adsorbing a small amount (0.1 L dose) of NO, which dissociates fully at low coverages²³ and results in equal amounts of N and O on the surface.

It is clear that dosing by the atom beam yields a higher N coverage than has been observed previously, but that there is a significant contamination from adsorbed O, particularly for

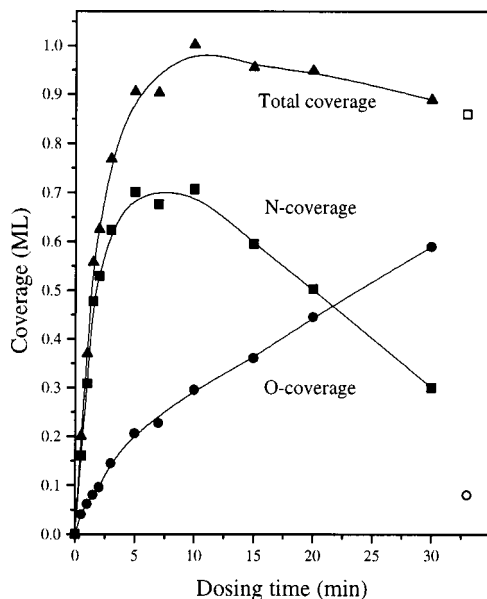


FIG. 1. N coverage, O coverage, and the total N+O coverage in ML/Ru atom as a function of N atom beam dose time. The open symbols refer to N and O coverages obtained after scrubbing [procedure (e) in Table I].

longer exposure times. For exposures beyond a few minutes, the sum of the N+O coverage is approximately unity. Since both preferentially occupy the same hcp 3-fold sites,²⁻⁵ it is reasonable that the combined coverage saturate at $\Theta=1$ since repulsive interactions between the adsorbates will certainly increase drastically beyond that coverage. It should also be noted that the maximum pure oxygen surface coverage obtainable is $\Theta_{\text{O}}=1$.⁷ The apparent displacement of N by O for high atom dosing is consistent with the stronger Ru–O bond compared to the Ru–N bonds (relative to associative desorption of the molecular O_2 or N_2). Our interpretation of these results is that although the atom beam has predominately N atoms, there is a small O atom impurity as well. Thus, the N+O atom coverage increases rapidly until the total coverage of N+O is 1. Then, the N is slowly displaced by the O impurity in the beam without increasing the total coverage of N+O.

For low atom beam doses, several of the well-known LEED structures for N adsorbed on Ru(0001) were observed. With increasing atom dose, the $p(2 \times 2)$ LEED pattern, the $(\sqrt{3} \times \sqrt{3})R-30^\circ$ LEED pattern, and that ascribed to the HDW structure were observed. For higher beam doses (>2 minutes dose time), no LEED structures other than the substrate (1×1) structure were observed, although there was considerable increase in the diffuse background indicating disorder of the surface adlayer.

In order to clarify the nature of a “pure” N adlayer, the O scrubbing procedure described before was employed to reduce the O contamination on the surface and to build up a higher coverage of N. A variety of different N coverages were produced on the surface with low O impurity by exposure to the N atom beam, followed by scrubbing with the H atom beam and then annealing to various T_s (all greater than 485 K). Because the anneal to 485 K limits the maximum N coverage due to thermal desorption of the adsorbed N, the

TABLE I. Summary of the experimental preparation procedures for the TPD spectra labeled (a)–(e) in Fig. 1. Values of Θ_{N} for each adlayer were obtained by comparing the N_2 TPD intensity to that from a saturated CO adlayer at $T_s=300$ K. Θ_{O} was obtained by the Auger intensity normalized to that for the $\Theta_{\text{O}}=0.5$ adlayer prepared by saturated O_2 background adsorption.

Experiment	Preparation procedure	Θ_{N}	Θ_{O}
(a)	2 min N atom beam exposure at $T_s=400$ K + 1 min H atom beam exposure at $T_s=400$ K + $T_s=630$ K surface anneal	0.29	0
(b)	2 min N atom beam exposure at $T_s=400$ K + 1 min H atom beam exposure at $T_s=400$ K + $T_s=535$ K surface anneal	0.38	0
(c)	2 min N atom beam exposure at $T_s=400$ K + 1 min H atom beam exposure at $T_s=400$ K + $T_s=500$ K surface anneal	0.54	0.02
(d)	2 min N atom beam exposure at $T_s=400$ K + 1 min H atom beam exposure at $T_s=400$ K + $T_s=485$ K surface anneal + 2 min N atom beam exposure at $T_s=300$ K	0.72	0.07
(e)	5 min N atom beam exposure at $T_s=400$ K + 2 min H atom beam exposure at $T_s=400$ K + $T_s=485$ K surface anneal + 4 min N atom beam exposure at $T_s=400$ K + 1.5 min H atom beam exposure at $T_s=400$ K + $T_s=485$ K surface anneal + 3 min N atom beam exposure at $T_s=300$ K	0.86	0.08

highest coverages were produced by following the above procedure with an additional final exposure to the N atom beam. This necessarily resulted in a small O atom impurity, but at much smaller levels than observed without scrubbing. The preparation recipe for various adlayers labeled (a) to (e), and their N atom and O atom coverages as determined by the procedures described previously, are given in Table I. For comparison with the dosing without scrubbing, the maximum N coverage obtained via this procedure and its O impurity are included in Fig. 1 as the open symbols.

TPD spectra for these lower impurity adlayers formed by the scrubbing are given in Fig. 2. Measurements of Θ_{N} are appended at the side of each TPD spectrum. The conditions for the preparation, Θ_{N} and Θ_{O} of the various adlayers are those given in Table I. In the TPD, we observe a series of desorption peaks filling sequentially with increasing N atom coverage in the adlayer. While clearly a given desorption peak does shift slightly with changes in N atom coverage, there seems to be five well defined peaks in the TPD spectra; 790 K, 635 K, 565 K, 500 K, and 430 K. There also appears to be a sharpening of the peaks for lower desorption temperatures. We attribute these results to associative desorption from a series of well defined states with different N coverage. The TPD spectra for a given adlayer showed no changes with time after the initial preparation. This indicates that the adsorbate structures probed during the TPD are at least metastable during the time scale of the experiments. Each TPD peak appears to saturate with N coverage before a new peak at lower T_s emerges. The preparation procedures (a)–(e) of Table I and Fig. 2 were chosen to approximately represent saturation of each successive peak without filling in the next

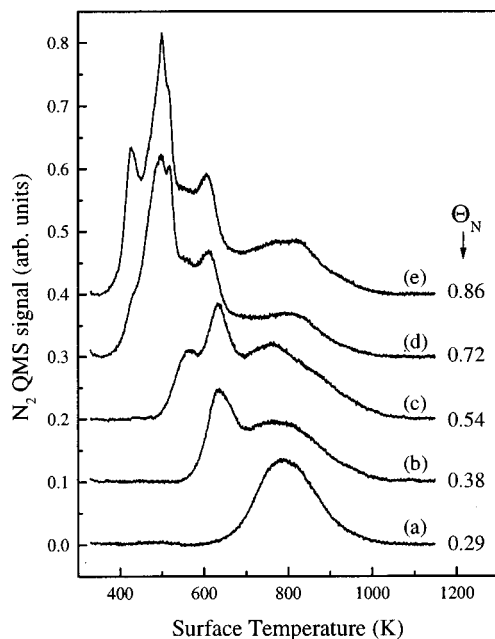


FIG. 2. N_2 TPD spectra for various coverages of nitrogen Θ_N adsorbed on Ru(0001). The preparation procedures for the curves labeled (a)–(e) are given in Table I.

lower T_s desorption peak. LEED studies indicated that preparation procedure (a) yielded a well defined $p(2 \times 2)$ pattern, procedure (b) gave a $(\sqrt{3} \times \sqrt{3})R-30^\circ$ pattern, and a coverage between (b) and (c) gave the HDW LEED pattern. Only very diffuse LEED patterns (other than the 1×1) were observed under preparation conditions (c)–(e) and no attempt was made to analyze them further. The TPD spectra from adlayers formed without the scrubbing were generally similar, except that intensities in the higher temperature N_2 TPD peaks decreased with exposure beyond ca. 2 min.

Assuming all desorption peaks are due to second-order associative desorption from the majority terrace sites, conventional Redhead analysis²⁴ allows us to estimate desorption energies (E_{des}) for each ‘‘state’’ from the desorption temperature peaks. These are given in Table II. These estimates used a preexponential for desorption for all states consistent with that obtained by Tsai and Weinberg²⁵ of $1.3 \times 10^{-3} \text{ cm}^2 \cdot \text{s}^{-1}$. The value of $E_{des} = 2.0 \text{ eV}$ obtained here for the lowest coverage state ($\Theta_N = 0.29$) is in good agreement with earlier experimental work; 1.91 eV (Ref. 25) and 1.97

TABLE II. Analysis of N_2 TPD spectrum in Fig. 2. Θ_N is the N atom coverage for the preparation procedures (a)–(e) outlined in the text and Table I, and obtained by a comparison to CO TPD intensities. These preparation procedures correspond approximately to the coverage where a given TPD feature fully saturates. E_{des} is the desorption energy calculated by a simple Redhead analysis for the given peak assuming second-order desorption kinetics.

TPD peak (K)	Θ_N	E_{des} (eV/molecule)
790	0.29	2.0
635	0.37	1.6
565	0.54	1.4
500	0.72	1.3
430	≥ 0.86	1.1

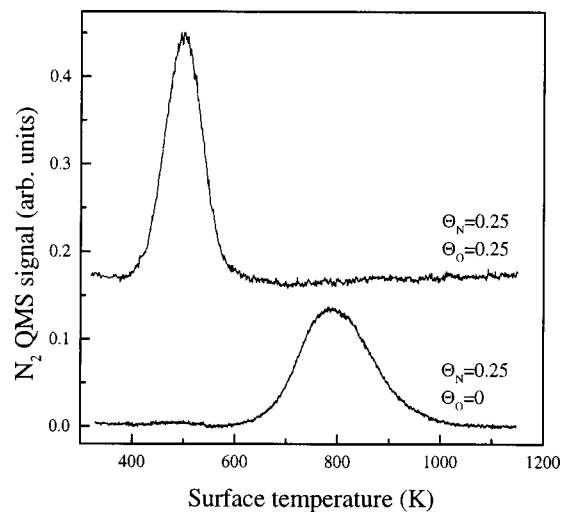


FIG. 3. N_2 TPD spectra for an initial nitrogen coverage $\Theta_N \approx 0.25$ without and with coadsorbed oxygen ($\Theta_O \approx 0.25$).

eV.¹³ As the coverage is increased we find a large decrease in E_{des} . Since it is entirely possible that the desorption is more like first-order (at the lower coverages) than second-order, we have also estimated desorption energies using first-order desorption and the preexponential of Tsai and Weinberg ($2 \times 10^{12} \text{ s}^{-1}$). These give E_{des} of 1.1, 1.3, 1.5, 1.7, and 2.1 eV for the various TPD peaks. All values are within 0.1 eV of those assuming 2nd order desorption. Thus the assumed order of desorption does not affect the overall conclusion that as the coverage is increased we find a large decrease in E_{des} .

Because of the high O impurity in the initial experiments at high coverage (before scrubbing was introduced), it was also interesting to measure the effects of coadsorbed O on the N associative desorption. Adsorption of N from the beam to $\Theta_N \approx 0.25$ followed by saturated background exposure to O_2 also produced a significant lowering of the N_2 associative desorption peak temperature as demonstrated in Fig. 3. Note, however, that there is only a single low T_s peak at $\approx 500 \text{ K}$ and no remaining desorption of N_2 at $T_s \approx 800 \text{ K}$ after dosing with O_2 . Under these exposure conditions, the total coverage was $\Theta_N + \Theta_O \approx 0.5$. The low N_2 associative desorption temperature of ca. 500 K when O is present on the surface has been observed several times previously, e.g., by thermal desorption following dissociative adsorption of NO on Ru(0001),²⁶ but has not been given any discussion or interpretation. No NO TPD was observed under these conditions.

DISCUSSION

Several low coverage states of N adsorbed on Ru(0001) have been previously well characterized experimentally. These include the $p(2 \times 2)$ -N, $\Theta_N = 0.25$ adlayer, the $(\sqrt{3} \times \sqrt{3})R-30^\circ$ -N, $\Theta_N = 0.33$ adlayer, and a higher coverage heavy domain wall structure (HDW) consisting of $(\sqrt{3} \times \sqrt{3})R-30^\circ$ -N patches with domain walls of local (1×1) -N structure, $\Theta_N = 0.36$ – 0.44 adlayer.^{14,15} The $p(2 \times 2)$ -N is the only stable structure at $T_s = 615 \text{ K}$, the $(\sqrt{3} \times \sqrt{3})R-30^\circ$ -N structure is produced at $T_s = 525 \text{ K}$, and

the HDW structure at $T_s=420$ K. LEED (Ref. 4) and STM (Ref. 23) studies demonstrate that N adsorbs in the HCP three-fold hollow site on the Ru(0001) surface for all known structures. The LEED experiments⁴ yield a N adsorption distance above the surface plane of ca. 1 Å and demonstrate that no substrate reconstruction and only modest relaxation occurs upon adsorption. STM experiments involving variable temperature anneals determined the indirect interactions between adsorbed N atoms.⁵ They obtained a repulsive N–N nearest- and second-nearest-neighbor interaction and an attractive third-nearest-neighbor interaction. With these indirect N–N interactions, they were able to rationalize all of the observed low coverage structures. Of particular importance for this work is that the authors conclude that the nearest-neighbor interaction must be quite repulsive, >0.2 eV. This means that any higher coverage states must be considerably less stable than those measured previously.

One curious aspect is that electron energy loss spectroscopy (EELS) studies indicate that the Ru–N vibrational frequency increases with coverage despite the fact that the energy/atom must decrease with coverage.^{13,14} A similar increase in the vibrational frequency with coverage has been observed for O/Ru(0001) vibrations and attributed to a steeper binding well due to repulsive O–O interactions, despite a lowering of the binding energy due to the same repulsive interaction.²⁷ Presumably, the same explanation is valid for N/Ru(0001) adlayers.

Our interpretation of the series of TPD spectra is that the broad highest temperature feature is desorption from low coverage up to and filling the well-known $p(2\times 2)$ adlayer of N adsorbed on Ru(0001) with $\Theta_N=0.25$. This assignment is in complete accord with all of the previous studies and was confirmed by the LEED measurements of preparation (a). The lower temperature peaks are interpreted as desorption from a series of higher coverage and less stable adlayers of adsorbed N. The TPD peak at 635 K is assigned as desorption from the $(\sqrt{3}\times\sqrt{3})R-30^\circ$ adlayer structure with $\Theta_N\approx 0.33$. This assignment agrees approximately with the measured Θ_N , with the anneal temperature necessary to produce this structure,¹⁴ and with the LEED measurements of preparation (b). Previous procedures (“filament assisted” adsorption or NH_3 dissociation) have not been able to resolve a well defined TPD peak for this state. In approximate agreement with measured Θ_N values, we tentatively assign the peak at 565 K to an adlayer with $\Theta_N\approx 0.5$, the peak at 500 K to an adlayer with $\Theta_N\approx 0.75$, and the peak at 430 K to the adlayer with $\Theta_N\approx 1$. None of these states have been observed previously and their structure is presently unknown. LEED studies at the higher coverages were inconclusive since at best very weak and diffuse additional LEED spots were observed. However, the sharp and well resolved TPD peaks do suggest the formation of moderately well defined adlayers at a given coverage. The assignment chosen facilitates comparison of the experimental results with theoretical calculations of coverage dependent adlayer stability. It is unlikely that any N adsorbs into subsurface sites since the observed N coverage (both by TPD and Auger) saturates when $\Theta_N+\Theta_O=1$. In addition, the scrubbing procedure which lowered the N coverage slightly, only diminished the lowest

TABLE III. Density functional theory calculations for average N atom adsorption energies E_N for an assumed adlayer structure of coverage Θ_N . Results are given as eV/atom relative to an origin given by the $1/2\text{N}_2+\text{Ru}(0001)$ asymptote. Results are quoted for calculations based on two different exchange correlation functionals (PW91 and RPBE) and based on the footnotes below. The RPBE results are anticipated to be more accurate.

Θ_N	E_N (eV/atom) PW91	E_N (eV/atom) RPBE
0.17	–0.62 ^a	–0.28 ^a
0.25	–0.65, ^a –0.77, ^b –0.7 ^c	–0.29 ^a
0.33	–0.47 ^c	–0.11 ^d
0.5	–0.24, ^a –0.19, ^b –0.2 ^c	+0.12 ^{a,c}
0.75	+0.2 ^c	+0.56 ^d
1.0	+0.5, ^a +0.6 ^c	+0.86 ^a

^aReference 16.

^bReference 6.

^cReference 4.

^dBased on estimating the RPBE adsorption energy from PW91 via $E_N(\text{RPBE})\approx E_N(\text{PW91})+0.36$ eV.

^eReference 9.

temperature TPD peak. Since scrubbing is a surface process (Eley–Rideal reaction with H), we infer that the lowest temperature TPD peak is due to repulsive interactions of species on the surface and not due to a subsurface feature.

Using “state of the art” density functional theory, the adsorption energies E_N for a series of known and (previously) unknown higher coverage N adsorbate states on the Ru(0001) have recently been calculated.^{4,6,9} Initial calculations were based on using the so-called PW91 exchange-correlation functional.^{4,6} It has recently been suggested that a slightly different functional, the so-called RPBE functional, gives improved adsorption energetics.²⁸ A summary of the DFT calculations is given in Table III. Calculations with both functionals predict the same important trend, i.e., that the binding energy decreases drastically with N coverage. Following Ref. 28, we assume that the RPBE calculations are more accurate and use these for comparison with our experiment. These show that the stability of the adsorbate states decreases drastically with N coverage, from -0.29 eV/N atom for $\Theta_N=0.25$ to $+0.86$ eV/N atom for $\Theta_N=1$, relative to the gas phase molecule. Thus states with $\Theta_N\geq 0.5$ are in fact not predicted to be thermodynamically stable on the surface. These calculations justify fully the qualitative concept of a strong indirect repulsive interaction due to the sharing of available Ru *d*-band electrons mentioned in the introduction. These DFT calculations are also in complete accord with the strong nearest-neighbor N–N repulsive interaction measured in the STM experiments.⁵ Since the high coverage states are not thermodynamically stable, it is not surprising that they had not been observed previously.

As mentioned in the introduction, the other dominate feature of $\text{N}_2/\text{Ru}(0001)$ interactions is the high barrier to dissociation. This barrier results in a very low dissociative sticking probability for background N_2 .^{9,29} The exact height of the barrier and the resulting thermal dissociation rate for N_2 on Ru surfaces has been somewhat controversial. Initial molecular beam experiments of N_2 dissociative sticking on Ru(0001) suggested a high dissociation barrier of ~ 2 eV,¹⁰ but the experimental data in this work are not consistent with

several newer, but as yet unpublished, molecular beam experiments.^{30–32} Thus, we are uncertain as to how to evaluate their experiment and conclusions. The thermal dependence of the rate of the N_2 dissociation on Ru(0001) at high pressures gives an activation barrier of only 0.4 eV on a reasonably good single crystal.⁹ However, if the (low density) natural steps on the surface are poisoned by coadsorption of Au, a much higher barrier of 1.3 eV is obtained.⁹ The authors suggest that the rate of dissociation in many experiments is dominated by the defects and that this may account for much of the discrepancy in comparing various measurements of dissociation rates. Another recent technique that has evolved to determine barrier heights (and other dynamic aspects) is to measure the translational energy (and internal state distribution) of molecules formed by associative desorption from the surface.^{33,34} Recent measurements of N_2 formed by associative desorption from Ru(0001) (Ref. 35) present a puzzling picture for the barrier since the energy dependence of the desorption flux peaks at low translational energies (consistent with a low barrier) but tails to high translational energies (consistent with a high barrier). The results are basically interpreted in terms of a very broad barrier distribution (energy dependent sticking function).

Some of the DFT calculations mentioned earlier have also probed the full minimum energy path to dissociation from gas phase N_2 to adsorbed N atoms at a total N/Ru coverage of 0.5.⁶ These calculations find a path which passes through the known molecularly adsorbed state ($E_M = -0.44$ eV/ N_2), through a metastable molecular state bonded parallel to the surface ($E_{MS} = 0.6$ eV/ N_2), through a barrier with a stretched N–N bond ($V^* = 1.36$ eV/ N_2) and into the N adsorbate state ($E_N = -0.77$ eV/N atom). All energies are relative to an origin defined by the infinitely separated $N_2 + Ru(0001)$. These initial calculations were based on using the PW91 exchange-correlation functional. Use of the improved RPBE functional gave a theoretical barrier height $V^* = 1.9$ eV.⁹

Thus, despite the contradictory experimental evidence, we agree with Ref. 9 that the barrier at low coverage is high, ≥ 1.4 eV, on terrace sites but that defects (steps, etc.) may significantly lower the barrier. We will show evidence below that the barrier actually increases significantly above this value of 1.4 eV at higher N coverage.

$E_{des}(\Theta_N)$ estimated from the thermal desorption experiments represents the energy difference between the adsorbate state and the barrier, $E_{des}(\Theta_N) = V^*(\Theta_N) - 2E_N(\Theta_N)$. Combining $E_{des}(\Theta_N)$ obtained here from the TPD measurements with $E_N(\Theta_N)$ from the DFT calculations allows predictions of $V^*(\Theta_N)$. This is shown in Fig. 4 and numerical values given in Table IV. It is immediately apparent in Fig. 4 (and Table IV) that V^* increases with Θ_N . The increase in $V^*(\Theta_N)$ is, however, less than the decrease in $E_N(\Theta_N)$. Of course, a shifting down of the desorption peak temperatures with Θ_N is the experimental consequence of this fact. Both the existence of this increase in V^* with Θ_N and the magnitude of its change relative to that of E_N are consistent with the explanation of the DFT calculations in terms of the necessity to share Ru d -band electrons at high N coverage. We will present elsewhere direct measurements of $V^*(\Theta_N)$ us-

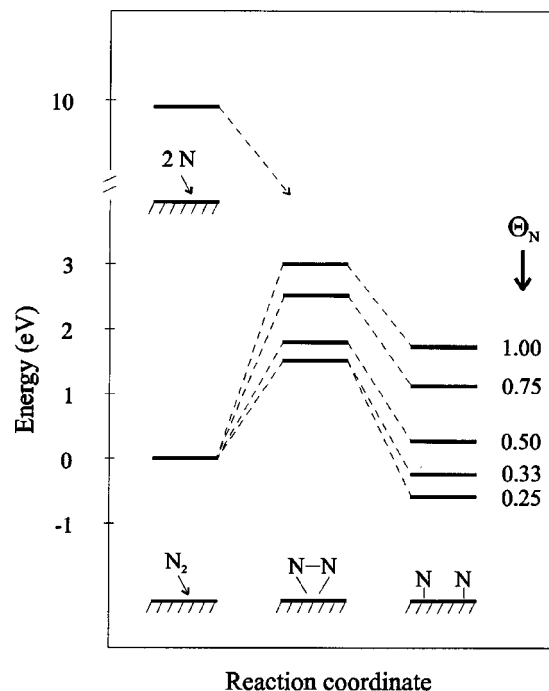


FIG. 4. Schematic energy diagram for the interaction of N_2 and $2N$ with the Ru(0001) surface. The origin of energy is taken as the $N_2 + Ru(0001)$ asymptote. The left side is the entrance channel for dissociative chemisorption. The right hand side is the atomic adsorbed state and is based on the DFT RPBE adsorption energies (see Table III). The center is the estimate of $V^*(\Theta_N)$ by combining the theoretical adsorption energies with the desorption energies obtained from the TPD (see Table II).

ing the technique of laser assisted associative desorption which confirm that the barriers increase substantially with Θ_N .³⁶

Figure 4 illustrates the difficulty in preparing the high coverage states. The prediction that states with $\Theta_N \geq 0.5$ are not thermodynamically stable relative to $N_2 + Ru(0001)$ means that it is difficult to prepare such states via N_2 dosing, even ‘‘filament assisted’’ adsorption since this process is endothermic. More importantly, the barrier to dissociative chemisorption increases substantially at higher coverage so that the energy cost for dissociating N_2 also increases. However, as Fig. 4 graphically illustrates, dissociating the N_2 in the gas phase provides more than enough energy to readily overcome all barriers and form all adsorbate states. The fact that the metastable high coverage states are observed via N

TABLE IV. Best estimates of coverage dependent N_2 dissociation barrier heights $V^*(\Theta_N)$ on Ru(0001) by combining TPD experiments and DFT calculations. $E_{des}(\Theta_N)$ from Table II assuming the TPD peaks correspond to desorption from $\Theta_N = 0.25, 0.33, 0.5, 0.75$ and 1, respectively. $E_N(\Theta_N)$ from Table III is based on the RPBE values. Barrier heights in eV are relative to the $N_2 + Ru(0001)$ asymptote.

Θ_N	$V^*(\Theta_N) = E_{des}(\Theta_N) + 2E_N(\Theta_N)$ (eV)
0.25	1.4
0.33	1.4
0.5	1.7
0.75	2.4
1.0	2.9

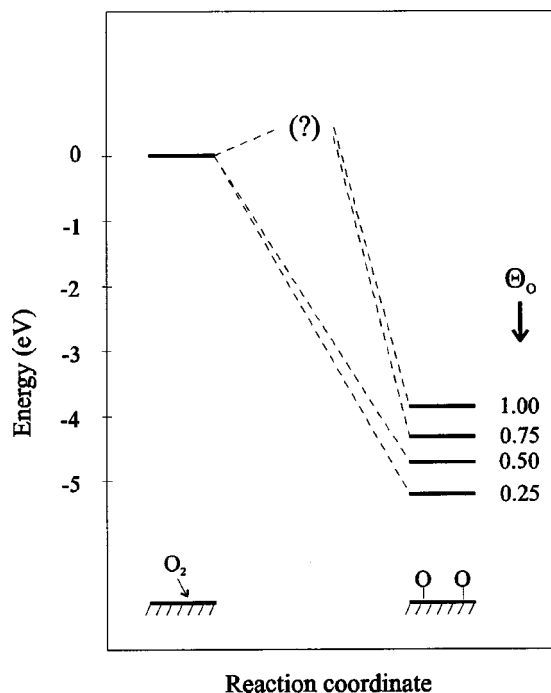


FIG. 5. Schematic energy diagram for the interaction of O_2 with Ru(0001). The adsorbed atomic state on the right side is based on DFT calculations of adsorption energies. For $\Theta_O=0.75$ and 1.0, the “kinetic barrier” is indicated as (?).

atom impingement at all and appear metastable for ≥ 30 min implies that they must have a significant surface lifetime.

It has recently been shown that the thermal activation energy for dissociative chemisorption of N_2 on Ru(0001) is lowered at step sites relative to terrace.⁹ By detailed balance, this may imply that the thermal desorption energies $E_{des}(\Theta_N)$ measured in the TPD experiments are those characteristic of desorption from the step sites. However, the relative importance of the steps vs terrace sites in the TPD experiments will depend in a complex way on the step density, coverage, diffusion rate to step sites, heating rate, etc. A model incorporating all these features is currently being developed. Even if the step sites do dominate thermal desorption, this merely implies that the desorption energies determined from the TPD experiments must be interpreted as lower limits to desorption energies from the terrace sites. If this is the case, then the barriers at the terraces may be somewhat higher than those of Fig. 4 and Table IV.

As mentioned in the introduction, the energetic and geometrical structure for a whole series of states of O adsorbed on Ru(0001) have also recently been studied.^{2,7} While the lower coverage $(2 \times 2)-O$, $\Theta_O=0.25$ and $(2 \times 1)-O$, $\Theta_O=0.5$ have long been known, newer work has demonstrated that $(2 \times 2)-3O$, $\Theta_O=0.75$ and $(1 \times 1)-O$, $\Theta_O=1$ are also stable on the surface.^{7,12} There is, however, a “kinetic barrier” to the formation of the $\Theta_O=0.75$ and $\Theta_O=1$ states so that either high pressures of O_2 or indirect methods (NO_2 dissociation) are necessary to prepare these states. The nature of this “kinetic barrier” is ill defined. It may just be a true energy barrier that occurs at high O coverage, in a similar manner as the energy barrier for N_2 dissociation increases with N coverage. However, since the dissociation is so exo-

thermic, the high coverage states are thermodynamically stable, in agreement with the DFT calculations. Figure 5 summarizes the energetics obtained for the O_2 /Ru(0001) system. It has also been observed that at sufficiently high exposures O atoms can be forced into subsurface sites.³⁷

Comparison of Fig. 5 with Fig. 4 highlights the similarities and differences between O_2 /Ru(0001) and N_2 /Ru(0001) interactions. As stated earlier, both dissociation processes are exothermic at low coverage to produce adsorbed atomic states on the surface. Because the O_2 bond is 4.6 eV weaker than the N_2 bond, the dissociation of O_2 on Ru(0001) is much more exothermic than that of N_2 , even though the Ru–N bond is 1.5 eV stronger than the Ru–O bond. Both systems support many different adsorbate states of different coverage up to a maximum coverage of $\Theta=1$. For the $(1 \times 1)-O$ structure, O occupies all available threefold HCP sites.⁷ Since N binds to Ru also in the threefold HCP sites at lower coverage,²³ we assume that the $(1 \times 1)-N$ structure also occupies all available threefold HCP sites as well. The binding energy decreases with Θ for each and this is described as an indirect repulsive interaction between the adsorbates due to the competition for available Ru *d*-band electron.^{6,38} We also see that since the binding energy decreases more rapidly for N than for O with coverage, the N–N indirect repulsive interaction between adsorbed species is stronger than that for O–O. This is interpreted as due to the fact that N has three valence electrons/atom interacting with the Ru *d*-bands instead of two for O. Hence, the competition for Ru-*d* electrons with coverage is enhanced. Because of the large exothermicity and modest indirect repulsive interaction, all adsorbate states of oxygen on Ru(0001) are thermodynamically stable. On the other hand, both because of the smaller exothermicity and larger adsorbate repulsive interactions, only low coverage states for nitrogen on Ru(0001) are thermodynamically stable. The relative strengths of the O_2 vs N_2 bonds is also fully in accord with the absence of a barrier to dissociation for O_2 at low coverage and the presence of a large barrier for N_2 dissociation. Both systems show, however, evidence that barriers increase with adsorbate coverage, although the nature of the barrier at high O coverage is not well characterized.

Given the discussion above about the similarities and differences between the N_2 +Ru(0001) and O_2 +Ru(0001) interactions, we can now rationalize the behavior of Fig. 3 where coadsorption of O shifts the TPD peak of the $\Theta_N=0.25$ state from $T_s=790$ K to $T_s=500$ K. Both O and N bind at the same HCP site. Therefore, the adlayer can exist in either phase separated domains or as mixed phases, depending upon details of all the lateral interactions. We have no way of knowing which situation exists at this total coverage ($\Theta_N+\Theta_O \approx 0.5$), although a low total coverage forms a mixed phase.³⁹ If the adlayer is phase separated, then the O coadsorbate merely compresses the N layer to patches of a local high coverage and this accounts for the lower peak desorption temperature. However, if a mixed phase exists, then the shifts of the desorption temperature must be due to a repulsive interaction by a coadsorbed O. Since both N–N and O–O exhibit indirect repulsive interactions that derive from the same physical origin (competition for Ru

d -electrons), we suggest that either neighbor can cause a local repulsive interaction to both the adsorption energy of adsorbed N and to V^* . Since we anticipate that shifts in E_N are greater than shifts in V^* , it is also anticipated that the desorption temperature for a given Θ_N would decrease with coadsorbed oxygen.

CONCLUSIONS

There has been considerable confusion as to the maximum coverage obtainable for N adsorbed on Ru(0001) and whether high coverage adsorbate states exist on this surface. Since the electronic interaction of N with Ru(0001) is similar to that of O with Ru(0001), and the latter supports a coverage $\Theta_O=1$, it is tempting to speculate that a state with $\Theta_N=1$ may also exist. In large part this has been unresolved due to experimental difficulties. There is a very high barrier for direct dissociation so that enormous exposures are required for N_2 and even “filament assisted” N_2 dosing. Indirect methods of preparation of a N adlayer (NH_3 or N_2H_4 dissociation, Eley–Rideal dissociation of NH_3 adsorbate by H ,⁴⁰ ion beam or electron beam dissociation of NH_3 adsorbate⁴¹ all require anneals to higher T_s to dissociate NH_x fragments. We report here a way to produce high coverage states of nitrogen atoms on Ru(0001) using an N atom beam formed by microwave discharge. Since the atom beam contains a considerable O atom impurity, it was necessary to “scrub” the O from the surface via an Eley–Rideal reaction with a gas phase atomic H beam. The results show that in fact a coverage of $\Theta_N \approx 1$ can be formed by atom dosing. A whole series of states of different coverage are observed on the surface as separate TPD peaks by varying the atom dose. The lowest coverage states agree with previous observations, but the higher ones are entirely new.

Density functional calculations (DFT) for N adsorbed on Ru(0001) (Refs. 4,6,9) indicate that the higher coverage states are in fact not stable relative to associative desorption. They must therefore be metastable, with a lifetime determined by the height of the barrier between gas phase N_2 and the adsorbed N states. Combination of our experimental TPD results with the DFT calculations allows us to estimate these coverage dependent barriers. We find that the barrier heights increase significantly with N coverage and this is in fact a necessary aspect of the metastability of the highest coverage states.

ACKNOWLEDGMENTS

The authors wish to thank the Danish Research Council for support of this work under Grant No. 9601724. L. D. and H. M. also wish to acknowledge support from the Danish Research Academy. We also thank A. Logadottir and J. K. Nørskov for providing us with their as yet unpublished calculations with the RPBE functional. The authors also wish to thank Surface Preparation Labs, Amsterdam for preparing the excellent quality Ru(0001) surface.

- ¹S. R. Tennison, in *Catalytic Ammonia Synthesis*, edited by J. R. Jennings (Plenum, New York, 1991), p. 303.
- ²C. Stampfl and M. Scheffler, *Phys. Rev. B* **54**, 2868 (1996).
- ³M. Lindroos, H. Pfnür, G. Held, and D. Menzel, *Surf. Sci.* **222**, 451 (1989).
- ⁴S. Schwegmann, A. P. Seitsonen, H. Dietrich, H. Bludau, H. Over, K. Jacobi, and G. Ertl, *Chem. Phys. Lett.* **264**, 680 (1997).
- ⁵J. Trost, T. Zambelli, J. Winterlin, and G. Ertl, *Phys. Rev. B* **54**, 17850 (1996).
- ⁶J. J. Mortensen, Y. Morikawa, B. Hammer, and J. K. Nørskov, *J. Catal.* **169**, 85 (1997).
- ⁷C. Stampfl, S. Schwegmann, H. Over, M. Scheffler, and G. Ertl, *Phys. Rev. Lett.* **77**, 3371 (1996).
- ⁸M. C. Wheeler, D. C. Seets, and C. B. Mullins, *J. Chem. Phys.* **105**, 1572 (1996).
- ⁹S. Dahl, A. Logadottir, R. C. Egeberg, J. H. Larsen, I. Chorkendorff, E. Törnqvist, and J. K. Nørskov, *Phys. Rev. Lett.* **83**, 1814 (1999).
- ¹⁰L. Romm, G. Katz, R. Kosloff, and M. Asscher, *J. Phys. Chem. B* **101**, 2213 (1997).
- ¹¹H. Pfnür, G. Held, M. Lindroos, and D. Menzel, *Surf. Sci.* **220**, 43 (1989).
- ¹²K. L. Kostov, M. Gsell, P. Jakob, T. Moritz, W. Widdra, and D. Menzel, *Surf. Sci.* **394**, L138 (1997).
- ¹³H. Shi, K. Jacobi, and G. Ertl, *J. Chem. Phys.* **99**, 9248 (1993).
- ¹⁴H. Dietrich, K. Jacobi, and G. Ertl, *J. Chem. Phys.* **105**, 8944 (1996).
- ¹⁵H. Rauscher, K. L. Kostov, and D. Menzel, *Chem. Phys. Phys. Phys.* **177**, 473 (1993).
- ¹⁶A. Logadottir and J. K. Nørskov (private communication).
- ¹⁷A. C. Luntz, M. D. Williams, and D. S. Bethune, *J. Chem. Phys.* **89**, 4381 (1988).
- ¹⁸R. A. Young, R. L. Sharpless, and R. Stringham, *J. Chem. Phys.* **40**, 117 (1964).
- ¹⁹S. N. Foner and R. L. Hudson, *J. Chem. Phys.* **37**, 1662 (1962).
- ²⁰K. R. Lykke and B. D. Kay, *J. Chem. Phys.* **95**, 2252 (1991).
- ²¹M. Schick, J. Wie, W. J. Mitchell, and W. H. Weinberg, *J. Chem. Phys.* **104**, 7713 (1996).
- ²²H. Pfnür, P. Feulner, and D. Menzel, *J. Chem. Phys.* **79**, 4613 (1983).
- ²³T. Zambelli, J. Trost, J. Winterlin, and G. Ertl, *Phys. Rev. Lett.* **76**, 795 (1996).
- ²⁴P. A. Redhead, *Vacuum* **12**, 203 (1962).
- ²⁵W. Tsai and W. H. Weinberg, *J. Phys. Chem.* **91**, 5302 (1987).
- ²⁶P. Jakob, M. Stichler, and D. Menzel, *Surf. Sci.* **370**, L185 (1997).
- ²⁷P. He and K. Jacobi, *Phys. Rev. B* **55**, 4751 (1997).
- ²⁸B. Hammer, L. B. Hansen, and J. K. Nørskov, *Phys. Rev. B* **59**, 7413 (1999).
- ²⁹H. Dietrich, P. Geng, K. Jacobi, and G. Ertl, *J. Chem. Phys.* **104**, 375 (1996).
- ³⁰J. H. Larsen, Ph.D. thesis, Technical University of Denmark, 1998.
- ³¹L. Diekhöner, H. Mortensen, A. Baurichter, and A. C. Luntz (unpublished).
- ³²A. Kleyn (private communication).
- ³³H. A. Michelsen, C. T. Rettner, and D. J. Auerbach, *Phys. Rev. Lett.* **69**, 2678 (1992).
- ³⁴M. J. Murphy and A. Hodgson, *J. Chem. Phys.* **108**, 4199 (1998).
- ³⁵M. J. Murphy, J. F. Skelly, A. Hodgson, and B. Hammer, *J. Chem. Phys.* **110**, 6954 (1999).
- ³⁶L. Diekhöner, H. Mortensen, A. Baurichter, A. C. Luntz, and B. Hammer (submitted).
- ³⁷A. Böttcher and H. Niehus, *J. Chem. Phys.* **110**, 3186 (1999).
- ³⁸J. J. Mortensen, B. Hammer, and J. K. Nørskov, *Surf. Sci.* **414**, 315 (1998).
- ³⁹C. Nagl, R. Schuster, S. Renisch, and G. Ertl, *Phys. Rev. Lett.* **81**, 3483 (1998).
- ⁴⁰C. J. Hagedorn, M. J. Weiss, and W. H. Weinberg, *J. Vac. Sci. Technol. A* **16**, 984 (1998).
- ⁴¹L. Danielson, M. J. Dresser, E. E. Donaldson, and D. R. Sandstrom, *Surf. Sci.* **71**, 615 (1978).